



**Faculty of Manufacturing Engineering**

**PREPARATION OF GRAPHENE/MOLYBDENUM DISULFIDE  
BASED ELECTRODES AND ITS ELECTROCHEMICAL  
PERFORMANCE IN SUPERCAPACITORS**

**Raja Noor Amalina binti Raja Seman**

**Doctor of Philosophy**

**2019**

**PREPARATION OF GRAPHENE/MOLYBDENUM DISULFIDE  
BASED ELECTRODES AND ITS ELECTROCHEMICAL PERFORMANCE IN  
SUPERCAPACITORS**

**RAJA NOOR AMALINA BINTI RAJA SEMAN**

**A thesis submitted  
in fulfilment of the requirements for the degree of Doctor of Philosophy**


**Faculty of Manufacturing Engineering**

**UNIVERSITI TEKNIKAL MALAYSIA MELAKA**

**2019**

## DECLARATION

I declare that this thesis entitled “Preparation of Graphene/Molybdenum Disulfide Based Electrodes and Its Electrochemical Performance in Supercapacitors” is the result of my own research except as cited in the references. The thesis has not been accepted for any degree and is not concurrently submitted in candidature of any other degree.

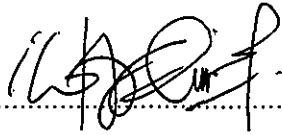
Signature :  .....

Name : Raja Noor Amalina binti Raja Seman

Date : 7/11/2019 .....

## APPROVAL

I hereby declare that I have read this thesis and in my opinion this thesis is sufficient in terms of scope and quality for the award of Doctor of Philosophy.

Signature : .....  
Supervisor Name : Assoc. Prof. Ir. Dr. Mohd Asyadi 'Azam bin Mohd Abid  
Date : 7 Nov. 2019.....

## **DEDICATION**

To my beloved family.

## ABSTRACT

Supercapacitor is highly promising energy device due to its electrical charge storage performance and significant lifecycle ability. Construction of the supercapacitor cell especially its electrode fabrication is critical to ensure great application performance. The purpose of this research is to fabricate the molybdenum disulfide ( $\text{MoS}_2$ ), graphene and G/ $\text{MoS}_2$  hybrid electrode and their usage as symmetric and asymmetric supercapacitors. The electrode was prepared by using a simple and facile slurry technique. By this, XRD was used to analyze the crystal phase and structure of the as-prepared graphene,  $\text{MoS}_2$ , and G/ $\text{MoS}_2$  hybrid. The peaks at  $14.3^\circ$ ,  $33.8^\circ$ , and  $57.5^\circ$  are attributed to the (002), (100), and (110) plane of  $\text{MoS}_2$  crystal. From Raman spectroscopy shows the characteristic peaks of graphene (D, G and 2D) and  $\text{MoS}_2$  ( $E_{2g}^1$  band at  $377\text{ cm}^{-1}$  and  $A_{1g}$  band at  $403\text{ cm}^{-1}$ ) are retained in the Raman spectra of G/ $\text{MoS}_2$  which can confirm the fact that the hybrid of G/ $\text{MoS}_2$  is composed of  $\text{MoS}_2$  and graphene. Next, the XPS analysis was carried out to deduce the exact elemental composition of the G/ $\text{MoS}_2$ . The full scan of the G/ $\text{MoS}_2$  gives the characteristic peaks for Mo 3d, S 2p, C 1s and O 1s with their corresponding binding energies. The morphologies and microstructures of the  $\text{MoS}_2$ , graphene and G/ $\text{MoS}_2$  are systematically characterized by FESEM observation. The high resolution of FESEM image further reveals that the  $\text{MoS}_2$  structures are constructed with layers of nanosheets. Meanwhile, FESEM image of graphene sheets illustrating the uniformly distributed of graphene into the Ni foam. Also, the inclusion of  $\text{MoS}_2$  nanosheets resulted in a rough surface, logically due to co-stacking of  $\text{MoS}_2$  nanosheets over the graphene nanosheets. Further, the morphology of the G/ $\text{MoS}_2$  was examined by TEM and reveals the crystal lattice structure of  $\text{MoS}_2$  and graphene in G/ $\text{MoS}_2$ . The interlayer spacing of  $\text{MoS}_2$  in the hybrid were estimated to be  $\sim 0.63\text{ nm}$ , which can be indexed to their (002) lattice planes of hexagonal phase of  $\text{MoS}_2$ . Regardless of the difference in electrode being used, cyclic voltammetry (CV) analysis from the supercapacitor depicted a relatively good specific gravimetric capacitance ( $C_{sp}$ ) and rate capability performance. A nearly rectangular-shaped CV curve was observed even at high scan rate. Besides, from the charge-discharge measurement, the symmetrical triangular curves reveal that there is no IR drops or voltage drops because of low internal resistance in the electrodes. Also, the electrode shows excellent discharge behavior and good capacitance retention of up to 10,000 cycles. Thus, this 2D heterostructures may provide excellent rate capabilities, high capacitance, and long lifecycle energy device. This is very promising for the development of high energy and high power density of device for multi-scale applications or industries.

## ABSTRAK

Superkapasitor adalah peranti tenaga yang sangat menarik kerana prestasi penyimpanan cas elektrik dan keupayaan kitaran hayat yang penting. Pembinaan sel superkapasitor terutamanya fabrikasi elektrod adalah penting untuk memastikan prestasi aplikasi yang hebat. Tujuan penyelidikan ini adalah untuk menyediakan elektrod molibdenum disulfida ( $\text{MoS}_2$ ), grafin dan hybrid  $\text{G}/\text{MoS}_2$  dan penggunaannya sebagai superkapasitor simetri dan asimetrik. Elektrod telah disediakan dengan menggunakan teknik campuran separa cair yang mudah dan senang. Dengan ini, XRD digunakan untuk menganalisis fasa kristal dan struktur grafin yang disediakan,  $\text{MoS}_2$ , dan hybrid  $\text{G}/\text{MoS}_2$ . Puncak pada  $14.3^\circ$ ,  $33.8^\circ$  dan  $57.5^\circ$  dikaitkan dengan kristal  $\text{MoS}_2$  (002), (100), dan (110). Dari spektroskopi Raman menunjukkan puncak ciri-ciri grafin (D, G dan 2D) dan  $\text{MoS}_2$  (band  $E'_{2g}$  pada  $377\text{ cm}^{-1}$  dan  $A_{1g}$  pada  $403\text{ cm}^{-1}$ ) dikekalkan dalam spektrum Raman hybrid  $\text{G}/\text{MoS}_2$  yang dapat mengesahkan fakta bahawa hybrid  $\text{G}/\text{MoS}_2$  terdiri daripada  $\text{MoS}_2$  dan grafin. Seterusnya, analisis XPS dijalankan untuk menyimpulkan komposisi elemen sebenar hybrid  $\text{G}/\text{MoS}_2$ . Siaran penuh hybrid  $\text{G}/\text{MoS}_2$  memberikan puncak ciri untuk Mo 3d, S 2p, C 1s dan O 1s dengan tenaga mengikat yang sama. Morfologi dan mikrostruktur  $\text{MoS}_2$ , grafin dan hybrid  $\text{G}/\text{MoS}_2$  secara sistematik dicirikan oleh pemerhatian FESEM. Resolusi tinggi imej FESEM dengan lebih lanjut mendedahkan bahawa struktur  $\text{MoS}_2$  dibina dengan lapisan nano. Sementara itu, imej FESEM lembaran grafin yang menggambarkan gambarajah secara seragam ke dalam Ni. Juga, kemasukan lapisan nano  $\text{MoS}_2$  menyebabkan permukaan yang kasar, secara logiknya disebabkan oleh penyambungan lapisan nano  $\text{MoS}_2$  ke atas lapisan nano grafin. Tambahan lagi, morfologi hybrid  $\text{G}/\text{MoS}_2$  diperiksa oleh TEM dan mendedahkan struktur kristal  $\text{MoS}_2$  dan grafin dalam hybrid  $\text{G}/\text{MoS}_2$ . Jarak lapisan dalam  $\text{MoS}_2$  di dalam hybrid adalah dianggarkan  $\sim 0.63\text{ nm}$ , yang boleh diindeks ke permukaan (002) fasa heksagon  $\text{MoS}_2$ . Tanpa mengira perbezaan elektrod yang digunakan, analisa voltametri siklik (CV) dari superkapasitor menggambarkan kapasitan gravimetrik spesifik ( $C_{sp}$ ) dan prestasi kadar keupayaan yang agak baik. CV berbentuk persegi panjang hampir diperhatikan walaupun pada kadar imbasan tinggi. Di samping itu, dari pengukuran caj pelepasan, lengkung segitiga simetri mendedahkan bahawa tiada kejatuhan IR atau penurunan voltan kerana rintangan dalaman yang rendah dalam elektrod. Juga, elektrod menunjukkan tingkah laku pelepasan yang sangat baik dan pengekalan kapasiti yang baik sehingga 10,000 pusingan. Jadi, heterostruktur 2D ini boleh memberikan keupayaan kadar yang sangat baik, kapasitan yang tinggi, dan peranti tenaga kitaran hayat yang panjang. Ini sangat menjanjikan untuk pembangunan tenaga tinggi dan ketumpatan kuasa tinggi untuk aplikasi pelbagai skala atau industri.

## ACKNOWLEDGEMENTS

First and foremost, thanks to Allah for helping me to complete this thesis. I would like to express my sincere appreciation to my project supervisor, Assoc. Prof. Ir. Dr. Mohd Asyadi 'Azam bin Mohd Abid for the encouragement, advices, suggestions and guidance upon completing my research project.

I am grateful to Faculty of Manufacturing Engineering, Universiti Teknikal Malaysia Melaka especially my co-supervisor Dr. Syahriza binti Ismail, assistant engineers in the laboratory, and my friends for the help and tremendous support for my research. I would like to acknowledge JC and Mr. Remy from Metrohm Malaysia, for their help in the usage of Autolab AUT 50430 to measure electrochemical performance (EIS) for my sample used in this work.

Also, I would like to acknowledge the UTeM Zamalah Scheme for financial support during my PhD study.

Lastly, I am grateful to my parents, my siblings for the continuous support and encouragement for me to finish up my study. I love you all.



## TABLE OF CONTENTS

	PAGE
DECLARATION	
APPROVAL	
DEDICATION	
ABSTRACT	i
ABSTRAK	ii
ACKNOWLEDGEMENTS	iii
TABLE OF CONTENTS	iv
LIST OF TABLES	viii
LIST OF FIGURES	ix
LIST OF ABBREVIATIONS	xiii
LIST OF SYMBOLS	xiv
LIST OF PUBLICATIONS	xv
LIST OF AWARDS	xvii

### CHAPTER

<b>1. INTRODUCTION</b>	<b>1</b>
1.1 Background	1
1.2 Problem statements	4
1.3 Objectives	6
1.4 Scope	6
1.5 Significant of study	8
1.6 Thesis structure	8
<b>2. LITERATURE REVIEW</b>	<b>10</b>
2.1 Introduction	10
2.2 Energy storage devices	11
2.2.1 Conventional capacitors	11
2.2.2 Batteries	12
2.2.3 Supercapacitors	13
2.2.3.1 History of supercapacitor	15
2.2.3.2 Advantages of supercapacitor	15
2.2.3.3 Challenges of supercapacitor	17
2.2.4 Comparison of different energy storage devices	19
2.2.5 Main components in supercapacitor	20
2.3 Supercapacitor as energy storage device	22
2.3.1 Application of supercapacitor	22
2.3.1.1 Consumer applications	22
2.3.1.2 Industrial applications	23
2.3.1.3 Public sector applications	23
2.3.1.4 Public transport applications	24
2.3.2 Electrochemical double layer capacitor (EDLC)	25
2.3.2.1 Helmholtz model	25

2.3.2.2	Gouy-Chapman or diffuse model	26
2.3.2.3	Stern modification of the diffuse double layer	27
2.3.2.4	Double layer theory in supercapacitor	28
2.3.3	Pseudocapacitor	29
2.4	Construction of high energy density supercapacitor	30
2.4.1	Symmetric supercapacitor	32
2.4.2	Asymmetric supercapacitor	33
2.4.3	Li-ion hybrid supercapacitor	34
2.5	Selection of the electrode materials for ASC	35
2.5.1	Negative electrode materials or Anode (Carbon-based materials)	36
2.5.1.1	Activated carbon	37
2.5.1.2	Carbon nanotube	38
2.5.1.3	Graphene	40
2.5.2	Negative electrode materials or Anode (Metal oxides)	41
2.5.3	Negative electrode materials or Anode (Metal nitrides)	43
2.5.4	Positive electrode materials or Cathode (Conductive polymers)	44
2.5.5	Positive electrode materials or Cathode (Metal oxides)	45
2.5.5.1	Ruthenium oxide ( $\text{RuO}_2$ )	45
2.5.5.2	Manganese oxide ( $\text{MnO}_2$ )	46
2.5.5.3	Vanadium pentoxide ( $\text{V}_2\text{O}_5$ )	47
2.5.5.4	Nickel hydroxide ( $\text{Ni}(\text{OH})_2$ )	47
2.6	Challenges of ASC	48
2.7	Electrode materials for supercapacitor	49
2.7.1	Graphene as representative of carbon material	51
2.7.2	Structure and properties of graphene	52
2.7.3	Synthesis of graphene	53
2.7.4	Molybdenum disulfide as representative of transition metal dichalcogenides material	54
2.7.5	Structure and properties of $\text{MoS}_2$	55
2.7.6	Synthesis of $\text{MoS}_2$	57
2.7.7	Graphene hybrids with other 2D analogues	59
2.8	Electrolytes for supercapacitor	61
2.8.1	Aqueous electrolyte	62
2.9	Material characterizations of supercapacitor electrode	63
2.9.1	Phase identification analysis by using X-Ray Powder Diffraction (XRD)	64
2.9.2	Structural properties analysis from Raman spectroscopy	65
2.9.3	Surface chemical state analysis by using X-Ray Photoelectron Spectroscopy (XPS)	66
2.9.4	Surface morphological analysis by using Field Emission Scanning Electron Microscopy (FESEM)	67

2.9.5	Morphological analysis by using Transmission Electron Microscopy (TEM)	68
2.10	Electrochemical performances of supercapacitor electrode	69
2.10.1	Cyclic Voltammetry (CV)	69
2.10.2	Galvanostatic Charge-Discharge (GCD)	70
2.10.3	Electrochemical Impedance Spectroscopy (EIS)	71
2.10.4	Determination of energy density and power density	73
2.11	Summary	75
<b>3.</b>	<b>METHODOLOGY</b>	<b>77</b>
3.1	Introduction	77
3.2	Flow chart of the experiment	78
3.3	Chemicals and laboratory apparatus	80
3.4	Preparation of G/MoS <sub>2</sub> hybrid electrode	82
3.4.1	Current collector preparation and cleaning	82
3.4.2	Optimization of PTFE binder ratio	84
3.4.3	Fabrication of MoS <sub>2</sub> , graphene, and G/MoS <sub>2</sub> hybrid electrodes	85
3.4.3.1	Determination of composition G/MoS <sub>2</sub> hybrid electrode	85
3.4.4	Types of aqueous electrolytes	86
3.5	Characterization and analysis of G/MoS <sub>2</sub> hybrid electrode	87
3.5.1	Crystallographic and molecular vibration using XRD, Raman spectroscopy, and XPS	88
3.5.1.1	X-Ray Diffraction (XRD)	88
3.5.1.2	Raman spectroscopy	88
3.5.1.3	X-Ray Photoelectron Spectroscopy (XPS)	88
3.5.2	Surface morphological analysis by using FESEM and TEM	89
3.6	Electrochemical performances of G/MoS <sub>2</sub> hybrid electrode	89
3.6.1	Cyclic Voltammetry (CV)	90
3.6.2	Galvanostatic Charge-Discharge (GCD)	91
3.6.3	Electrochemical Impedance Spectroscopy (EIS)	92
3.6.4	Determination of energy density and power density	92
3.7	Cell assembly of G/MoS <sub>2</sub> hybrid electrode	93
3.8	Summary	94
<b>4.</b>	<b>RESULT AND DISCUSSION</b>	<b>95</b>
4.1	Introduction	95
4.2	Preparation of electrode materials	96
4.2.1	Determination of PTFE binder ratio for supercapacitor	96
4.2.2	Optimization of G/MoS <sub>2</sub> hybrid supercapacitor	100

4.2.3	Structural and properties of MoS <sub>2</sub> , graphene, and G/MoS <sub>2</sub> hybrid electrodes	105
4.2.3.1	Phase identification of MoS <sub>2</sub> , graphene, and G/MoS <sub>2</sub> hybrid by using XRD	105
4.2.3.2	Structural properties of MoS <sub>2</sub> , graphene, and G/MoS <sub>2</sub> hybrid by using Raman spectroscopy	107
4.2.4	Surface chemical state of MoS <sub>2</sub> , graphene, and G/MoS <sub>2</sub> hybrid electrodes by using XPS	110
4.2.5	Morphological analyses of as-prepared MoS <sub>2</sub> , graphene, and G/MoS <sub>2</sub> hybrid electrodes	113
4.2.5.1	Observation by FESEM	113
4.2.5.2	Structural analysis of G/MoS <sub>2</sub> hybrid by using TEM	115
4.3	Electrochemical performances of MoS <sub>2</sub> , graphene, and G/MoS <sub>2</sub> hybrid supercapacitor	117
4.3.1	Symmetric supercapacitor in aqueous electrolytes for MoS <sub>2</sub> , graphene, and G/MoS <sub>2</sub> hybrid	119
4.3.1.1	Electrochemical performances of MoS <sub>2</sub> supercapacitor in 6M KOH, 1M H <sub>2</sub> SO <sub>4</sub> , and 0.5M Na <sub>2</sub> SO <sub>4</sub> electrolytes	120
4.3.1.2	Electrochemical performances of graphene supercapacitor in 6M KOH, 1M H <sub>2</sub> SO <sub>4</sub> , and 0.5M Na <sub>2</sub> SO <sub>4</sub> electrolytes	127
4.3.1.3	Electrochemical performances of G/MoS <sub>2</sub> hybrid supercapacitor in 6M KOH, 1M H <sub>2</sub> SO <sub>4</sub> , and 0.5M Na <sub>2</sub> SO <sub>4</sub> electrolytes	138
4.3.2	Asymmetric supercapacitor in aqueous electrolytes	151
4.3.2.1	Electrochemical performances of ASC G//MoS <sub>2</sub> electrodes in 6M KOH, 1M H <sub>2</sub> SO <sub>4</sub> , and 0.5M Na <sub>2</sub> SO <sub>4</sub> electrolytes	151
4.3.2.2	Electrochemical performances of ASC G//G/MoS <sub>2</sub> electrodes in 6M KOH, 1M H <sub>2</sub> SO <sub>4</sub> , and 0.5M Na <sub>2</sub> SO <sub>4</sub> electrolytes	160
4.3.3	Comparison of electrochemical performances of supercapacitors by using Ragone plot	168
4.4	Summary	172
<b>5.</b>	<b>CONCLUSION AND RECOMMENDATIONS</b>	<b>174</b>
5.1	Conclusion	174
5.2	Recommendations	176
	<b>REFERENCES</b>	<b>177</b>

## LIST OF TABLES

TABLE	TITLE	PAGE
2.1	Comparison between conventional capacitors, batteries, fuel cells, and supercapacitors (Bubna et al., 2012)	20
2.2	Capacitance value of electrode materials in different aqueous electrolytes	59
3.1	Materials for MoS <sub>2</sub> , graphene, and G/MoS <sub>2</sub> hybrid electrode fabrication	80
3.2	Equipment for MoS <sub>2</sub> , graphene, and G/MoS <sub>2</sub> hybrid electrode fabrication	81
3.3	Current collector information	82
3.4	The amount of graphene and MoS <sub>2</sub> composition	85
3.5	The sizes of bare and hydrated ions, and ionic conductivity values (Zhong et al., 2015)	87
3.6	Cyclic voltammetry parameter	90
3.7	GCD parameter	91
4.1	Slurry composition of graphene electrodes	97
4.2	$C_{sp}$ of graphene electrodes with different ratio of PTFE binder	98
4.3	The G/MoS <sub>2</sub> hybrid electrodes description	101
4.4	$C_{sp}$ of G/MoS <sub>2</sub> hybrid electrodes calculated from CV	103
4.5	$C_{sp}$ of G/MoS <sub>2</sub> hybrid electrodes calculated from GCD at 1 mA	105
4.6	Calculation of average weight of MoS <sub>2</sub> , graphene, G/MoS <sub>2</sub> , G//MoS <sub>2</sub> , and G//G/MoS <sub>2</sub> hybrid electrodes	118
4.7	$C_{sp}$ (in F g <sup>-1</sup> ) for MoS <sub>2</sub> , graphene, and G/MoS <sub>2</sub> electrodes from CV analyses	141
4.8	$C_{sp}$ (in F g <sup>-1</sup> ) for ASC G//MoS <sub>2</sub> and ASC G//G/MoS <sub>2</sub> electrodes from CV analyses	165

## LIST OF FIGURES

FIGURE	TITLE	PAGE
1.1	Molybdenum disulfide atomic structure (He and Que, 2016)	1
1.2	An example of hydrothermal process and G/MoS <sub>2</sub> heterostructures formation mechanism (Yang et al., 2017)	3
2.1	The drawing of schematic diagram of conventional capacitor	11
2.2	The drawing of charging-discharging in LIB	13
2.3	(a) The mechanism of CD process for EDLC and (b) energy storage mechanism for pseudocapacitor (Jost et al., 2014)	14
2.4	Common symmetric electrode cell component for supercapacitor	21
2.5	Helmholtz model (Pilon et al., 2015)	26
2.6	Gouy-Chapman or diffuse model (Pilon et al., 2015)	27
2.7	Stern modification of the diffuse double layer (Pilon et al., 2015)	28
2.8	Schematic illustration of the as-fabricated asymmetric supercapacitor (ASC) device based on manganese sulfide (MnS) nanocrystal as the positive electrode and EDAC as the negative electrode (Chen et al., 2016)	31
2.9	The drawing of symmetric supercapacitor	32
2.10	The drawing of ASC	34
2.11	The drawing of Li-ion supercapacitor	35
2.12	Several forms of carbon nanostructures (Al-Jumaili et al., 2017)	39
2.13	Schematics of CVD graphene grown on (a) metals with high carbon solubility, (b) Copper foil, (c) Copper enclosure, and (d) sapphire (Chen et al., 2015)	54
2.14	(a) TMDs crystal structures of MX <sub>2</sub> . (b) Three-dimensional model of the MoS <sub>2</sub> crystal structure in 1T and 2H types (Lv et al., 2015)	57
2.15	Schematic representation of the electrochemical lithiation process for synthesis of 2D nanosheets from layered bulk materials (Chhowalla et al., 2013)	58
2.16	Variety of electrolytes for supercapacitors	63
2.17	XRD patterns of 3DG, MoS <sub>2</sub> and GS-5 (Sun et al., 2016)	65
2.18	Raman spectra of GO, pure MoS <sub>2</sub> , and MoS <sub>2</sub> /graphene composites (Thangappan et al., 2016)	66
2.19	High resolution XPS spectra of MoS <sub>2</sub> raw powder showing the S 2p (a) and Mo 3d (b) binding regions (Bissett et al., 2015)	67

2.20	SEM images of the G/MoS <sub>2</sub> composite (a and b), pristine graphene (c) (Thangappan et al., 2016)	68
2.21	TEM images of graphene (A), and MoS <sub>2</sub> -graphene composites (B); HRTEM image of MoS <sub>2</sub> -graphene composites (Huang et al., 2013)	68
2.22	CV curves of (A) MoS <sub>2</sub> particles and (B) hierarchical MoS <sub>2</sub> /G nanobelts at different scan rates (C) CV curves of the electrodes at 10 mV s <sup>-1</sup> (D) areal capacitances of the electrodes at different scan rates (Jia et al., 2017)	70
2.23	GCD curves of MoS <sub>2</sub> -graphene composites at different current densities (1, 2.5, 5 and 10 A g <sup>-1</sup> ) (Huang et al., 2013)	71
2.24	Nyquist plots of the MoS <sub>2</sub> , graphene and MoS <sub>2</sub> -graphene composites electrode in 1.0 M Na <sub>2</sub> SO <sub>4</sub> in the frequency range from 0.1 to 100 kHz at open circuit potential with an ac perturbation of 5 mV. Inset: magnified high frequency regions (Huang et al., 2013)	72
2.25	Ragone plot for various energy storage devices (Simon and Gogotsi, 2008)	73
3.1	Flow chart of experiment	79
3.2	A piece of current collector with 15 mm diameter	82
3.3	Schematic illustration of G/MoS <sub>2</sub> hybrid slurry coated onto Ni foam	82
3.4	Ni foam cleaning process flow	84
3.5	(a) Major components of supercapacitor, and (b) illustration of G/MoS <sub>2</sub> hybrid electrode inside con cell	93
4.1	CV curves in a potential range of 0.0-1.0 V at different scan rates in 6M KOH electrolyte	98
4.2	GCD curves at different currents for three different ratio	99
4.3	Cycling stability tested at applied current of 3 mA in 6M KOH electrolyte	100
4.4	CV curves for five different compositions at 1–60 mV s <sup>-1</sup>	102
4.5	CD curves for five different compositions at 0.6 to 1 mA in 6M KOH electrolyte	104
4.6	XRD patterns of MoS <sub>2</sub> , graphene, and G/MoS <sub>2</sub> hybrid	106
4.7	Raman spectra of MoS <sub>2</sub> , graphene, and G/MoS <sub>2</sub> hybrid	107
4.8	Wide range XPS spectra of G/MoS <sub>2</sub> hybrid	110
4.9	XPS spectra of C 1s of G/MoS <sub>2</sub> hybrid	111
4.10	XPS spectra of Mo 3d of G/MoS <sub>2</sub> hybrid	112
4.11	XPS spectra of S 2p of G/MoS <sub>2</sub> hybrid	112
4.12	FESEM image of MoS <sub>2</sub>	113
4.13	FESEM image of graphene sheet	114
4.14	FESEM image of G/MoS <sub>2</sub> hybrid	115
4.15	TEM image of G/MoS <sub>2</sub> hybrid	116
4.16	CV of MoS <sub>2</sub> electrodes at scan rate 1 mV s <sup>-1</sup> in three different electrolytes measured from 0.0 to 1.0 V	121

4.17	CV of MoS <sub>2</sub> electrodes at various scan rates in three different electrolytes measured from 0.0 to 1.0 V	122
4.18	CD curves of MoS <sub>2</sub> electrodes at three different electrolytes	124
4.19	Capacitance retention of MoS <sub>2</sub> electrodes over 10, 000 charge/discharge cycles	125
4.20	EIS Nyquist plots of MoS <sub>2</sub> electrodes in three different electrolytes	126
4.21	CV of graphene electrodes at scan rate 1 mV s <sup>-1</sup> in three different electrolytes measured from 0.0 to 1.0 V	128
4.22	CV of graphene electrodes at various scan rates in three different electrolytes measured from 0.0 to 1.0 V	130
4.23	CD curves of graphene electrodes at three different electrolytes	133
4.24	Capacitance retention of graphene electrodes over 10, 000 charge/discharge cycles	135
4.25	EIS Nyquist plots of graphene electrodes in three different electrolytes	136
4.26	CV of G/MoS <sub>2</sub> hybrid electrodes at scan rate 1 mV s <sup>-1</sup> in three different electrolytes measured from 0.0 to 1.0 V	139
4.27	CV of G/MoS <sub>2</sub> hybrid electrodes at various scan rates in three different electrolytes measured from 0.0 to 1.0 V	140
4.28	CD curves of G/MoS <sub>2</sub> hybrid electrodes at three different electrolytes	145
4.29	Capacitance retention of G/MoS <sub>2</sub> hybrid electrodes over 10, 000 charge/discharge cycles	148
4.30	EIS Nyquist plots of G/MoS <sub>2</sub> hybrid electrodes in three different electrolytes	150
4.31	CV of ASC G//MoS <sub>2</sub> electrodes at scan rate 1 mV s <sup>-1</sup> in three different electrolytes measured from 0.0 to 1.2 V	152
4.32	CV of ASC G//MoS <sub>2</sub> electrodes at various scan rates in three different electrolytes measured from 0.0 to 1.2 V	153
4.33	CD curves of ASC G//MoS <sub>2</sub> electrodes at three different electrolytes	155
4.34	Capacitance retention of ASC G//MoS <sub>2</sub> electrodes over 10, 000 charge/discharge cycles	156
4.35	EIS Nyquist plots of ASC G//MoS <sub>2</sub> electrodes in three different electrolytes	158
4.36	CV of ASC G//G/MoS <sub>2</sub> electrodes at scan rate 1 mV s <sup>-1</sup> in three different electrolytes measured from 0.0 to 1.2 V	161
4.37	CV of ASC G//G/MoS <sub>2</sub> electrodes at various scan rates in three different electrolytes measured from 0.0 to 1.2 V	162
4.38	CD curves of ASC G//G/MoS <sub>2</sub> electrodes at three different electrolytes	164
4.39	Capacitance retention of ASC G//G/MoS <sub>2</sub> hybrid electrodes over 10, 000 charge/discharge cycles	165



4.40	EIS Nyquist plots of ASC G//G/MoS <sub>2</sub> electrodes in three different electrolytes	167
4.41	Ragone plots of MoS <sub>2</sub> , graphene, G/MoS <sub>2</sub> hybrid symmetric supercapacitors and G//MoS <sub>2</sub> and G//G/MoS <sub>2</sub> ASCs	169

## LIST OF ABBREVIATIONS

AC	-	Activated Carbon
ASC	-	Asymmetric Supercapacitor
CNT	-	Carbon Nanotube
CP	-	Conducting Polymer
$C_{sp}$	-	Specific Gravimetric Capacitance
CV	-	Cyclic Voltammetry
CVD	-	Chemical Vapor Deposition
ED	-	Energy Density
EDLC	-	Electrochemical Double Layer Capacitor
EIS	-	Electrochemical Impedance Spectroscopy
FESEM	-	Field Emission Scanning Electron Microscopy
G	-	Graphene
GCD	-	Galvanostatic Charge-Discharge
$H_2SO_4$	-	Sulfuric Acid
KOH	-	Potassium Hydroxide
LIB	-	Lithium Ion Battery
$MoS_2$	-	Molybdenum Disulfide
$Na_2SO_4$	-	Sodium Sulfate
NMP	-	N-Methyl-2-pyrrolidone
PTFE	-	Polytetrafluoroethylene
TEM	-	Transmission Electron Microscopy
TMD	-	Transition Metal Dichalcogenide
XRD	-	X-Ray Powder Diffraction
XPS	-	X-Ray Photoelectron Spectroscopy
2D	-	Two Dimensional

## LIST OF SYMBOLS

$F g^{-1}$	-	Farad per gram
$g$	-	Gram
$k$	-	Kilo
$m$	-	Meter
$e$	-	Electron
$mA$	-	MiliAmpere
$mV s^{-1}$	-	MiliVolts per second
$\mu m$	-	Micrometer
$nm$	-	Nanometer
$Pa$	-	Pascal
$s$	-	Second
$W kg^{-1}$	-	Watts per kilogram
$Wh kg^{-1}$	-	Watts hour per kilogram
$^{\circ}C$	-	Degree celcius
$V$	-	Voltage
$W$	-	Watt
$CV$	-	Cyclic voltammetry
$\Psi_0$	-	Electrode potential
$\Psi$	-	Potential

## LIST OF PUBLICATIONS

### (i) Peer reviewed journals

1. Seman, R.N.A.R., Azam, M.A. and Ani, M.H., 2018. Graphene/transition Metal Dichalcogenides Hybrid Supercapacitor Electrode: Status, Challenges, and Perspectives. *Nanotechnology*, 29(50), pp. 502001–502025.
2. Azam, M.A., Talib, E. and Seman, R.N.A.R., 2018. Direct Deposition of Multi-Walled Carbon Nanotubes onto Stainless Steel and YEF foils using a Simple Electrophoretic Deposition for Electrochemical Capacitor Electrode. *Materials Research Express*, 6(1), pp. 015501–015508.
3. Azam, M.A., Mudtalib, N.E.S.A.A. and Seman, R.N.A.R., 2018. Synthesis of Graphene Nanoplatelets from Palm-Based Waste Chicken Frying Oil Carbon Feedstock by Using Catalytic Chemical Vapour Deposition. *Materials Today Communications*, 15, pp. 81–87.
4. Lau, K.T., Azam, M.A. and Seman, R.N.A.R., 2018. Influence of Pulsed Electrophoretic Deposition of Graphitic Carbon Nanotube on Electrochemical Capacitor Performance. *Journal of Engineering Science and Technology*, 13(2), pp. 295–308.
5. Azam, M.A., Seman, R.N.A.R., Zulkifli, M.F., Mohamed, M.A. and Ani M.H., 2018. Carbon Nanomaterials Derived from Malaysia's Highway Road Asphalt Waste as Electrode for Supercapacitor. *Journal of Materials and Environmental Sciences*, 9 (7), pp. 2164–2168.
6. Azam, M.A., Seman, R.N.A.R. and Effendi S.M., 2017. Preparation of Hydrous Ruthenium Oxide/Activated Carbon Electrode and Its Supercapacitive Performance in 6M KOH. *Journal of Advanced Manufacturing Technology (JAMT)*, 11(2), pp. 1–8.
7. Azam, M.A., Alias, F.M., Tack, L.W., Seman, R.N.A.R. and Taib, M.F.M., 2017. Electronic Properties and Gas Adsorption Behaviour of Pristine, Silicon-, and Boron-Doped (8, 0) Single-Walled Carbon Nanotube: A First Principles Study. *Journal of Molecular Graphics and Modelling*, 75, pp. 85–93.
8. Seman, R.N.A.R., Azam, M.A. and Mohamad, A.A., 2017. Systematic Gap Analysis of Carbon Nanotube-Based Lithium-Ion Batteries and Electrochemical Capacitors. *Renewable and Sustainable Energy Reviews*, 75, pp. 644–659.

9. Tack, L.W., Azam, M.A. and Seman, R.N.A.R., 2017. Structural and Electronic Properties of Transition-Metal Oxides Attached to a Single-Walled CNT as a Lithium-Ion Battery Electrode: A First-Principles Study. *The Journal of Physical Chemistry A*, 121 (13), pp. 2636–2642.
10. Azam, M.A., Zulkapli, N.N., Dorah, N., Seman, R.N.A.R., Ani, M.H., Sirat, M.S., Ismail, E., Fauzi, F.B., Mohamed, M.A. and Majlis, B.Y., 2017. Critical Considerations of High Quality Graphene Synthesized by Plasma-Enhanced Chemical Vapor Deposition for Electronic and Energy Storage Devices. *ECS Journal of Solid State Science and Technology*, 6(6), pp. M3035–M3048.
11. Seman, R.N.A.R., Azam, M.A. and Mohamed M.A., 2016. Highly Efficient Growth of Vertically Aligned Carbon Nanotubes on Fe–Ni Based Metal Alloy Foils for Supercapacitors. *Advances in Natural Sciences: Nanoscience and Nanotechnology*, 7(4), pp. 045016–045024.

(ii) Conference presentation

1. Electrochemical performance of molybdenum disulfide Supercapacitor Electrode in potassium hydroxide and sodium sulfate electrolytes, 5th International Conference and Exhibition on Sustainable Energy and Advanced Materials Holiday Inn Melaka, 16–19 October 2017 (Oral presentation).
2. Effects of PTFE binder ratio on the performance of graphene supercapacitor, ISoRIS'17, Ramada Hotel, Melaka, 18 & 19 July 2017 (Oral presentation).

## LIST OF AWARDS

1. 29th International Invention, Innovation & Technology Exhibition 2018

Place: KLCC Convention Centre Kuala Lumpur

Date: 10–12 May 2018

ITEX 2018 Silver medal

2. UTeM Research and Innovation Expo (UTeMEX)

Date: 17 November 2017

Place: FTK Universiti Teknikal Malaysia Melaka

Jury Special award & Gold award

3. Seoul International Invention Fair (SIIF 2016)

Date: 1–2 December 2016, Korea

Place: Seoul, Korea

Silver Medal

4. Malaysia Technology Expo 2016 (MTE 2016)

Date: 18–20 February 2016

Place: PWTC Kuala Lumpur

Special Award & Gold Award

# CHAPTER 1

## INTRODUCTION

### 1.1 Background

Currently new electrode materials are under intense study to be used in supercapacitor applications, including transition metal oxides, metal hydroxides, and conducting polymers. Compared with other electrode materials such as carbon based materials, these electrode materials give high capacitance. Despite having high capacitance, these electrode materials possess low electrical conductivity, leading to inferior cycling stability as well as lower energy and power densities.

Graphene, composed of carbon atoms arranged in a honeycomb lattice, has been shown to possess unique properties. Additionally, the transition metal chalcogenide molybdenum disulfide ( $\text{MoS}_2$ ) (Figure 1.1) shows prospects for various applications, including supercapacitors, because of the unique atomic structure analogues with graphene (Cao et al., 2013; Hu et al., 2013; Shi et al., 2013; He and Que, 2016).

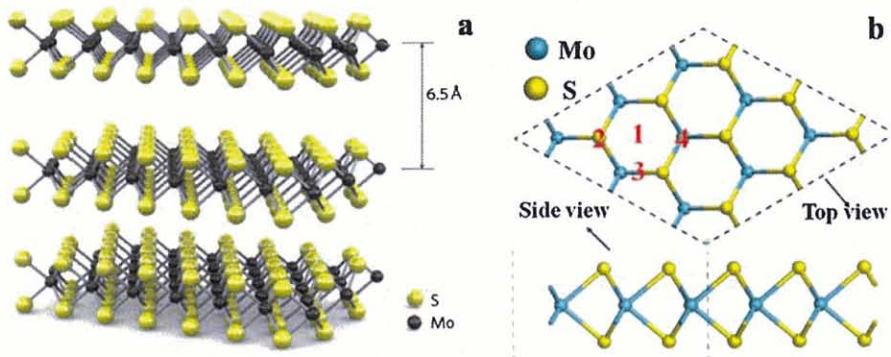


Figure 1.1: Molybdenum disulfide atomic structure (He and Que, 2016)

Research into green and renewable energy materials is expanding, as well as the market for low cost and light-weight electrochemical energy storage systems. Among energy

storage devices, supercapacitors are one of the most popular energy storage devices contrasted with batteries because of their long life stabilities, fast charge-discharge processes, and high power density (Lu et al., 2013a).

Fabrication of superior electrode materials with well design structures is a crucial factor to increase high electrochemical performance of the energy storage devices such as high energy density an

d high power density (Cakici et al., 2017; Chen et al., 2017). Layered MoS<sub>2</sub> is analogous to the two-dimensional (2D) structure of graphene. The intercalation of electrolyte ions is permitted from the usage of MoS<sub>2</sub> as an electrode material in supercapacitors.

Thus, the key factor that determines the storage mechanism of supercapacitor is the diameter of electrolyte ion as well as matching of the interlayer spacing (Zhou et al., 2017). The construction of 2D hybrid heterostructures of graphene and MoS<sub>2</sub> (G/MoS<sub>2</sub>) is believed to allow strongly coupled nanohybrid materials with optimized functionalities for supercapacitor application.

In addition, chemical vapor deposition (CVD), reduction-induced in situ self-assembly, chemical assembly, and the hydrothermal method (Figure 1.2) are simple methods which provide a unique approach for the synthesis of G/MoS<sub>2</sub> for energy storage applications (Yang et al., 2017). These novel materials and the fabrication of symmetric and asymmetric supercapacitors are important in meeting energy and power demands.

Asymmetric supercapacitors (ASCs) are composed of two dissimilar electrodes such as carbon and pseudocapacitive materials based electrodes (Wu et al., 2014; Sun et al., 2015). Commonly, the negative electrode in ASC is composed of carbon based materials including graphene, carbon nanotube, and activated carbon. Meanwhile, metal oxides and conducting polymers are the example of the positive electrode in ASC.